# Observational constraints on dissipative Chaplygin gas cosmology in the framework of coincident $f(Q)$ gravity*

Sayantan Ghosh[1†] Raja Solanki[2‡] P. K. Sahoo[1§]

[1]Department of Mathematics, Birla Institute of Technology and Science, Telangana 500078, India
[2]Department of Mathematics, School of Advanced Sciences, VIT-AP University, Amaravati 522241, India

**Abstract:** In this study, we shed light on the unified approach to dark energy and dark matter via the generalized Chaplygin gas model in symmetric teleparallel gravity (STGR). We employ the equation of state provided by generalized Chaplygin gas, which naturally arises in string theory, tachyonic field theory, and Randall-Sundrum-type brane world solutions. Such a generalized Chaplygin gas not only provides a viable candidate for dark energy but also for dark matter via Bose-Einstein condensation (BEC). We also consider the interaction between dark matter and dark energy to provide a more realistic perspective. Moreover, we perform Markov Chain Monte Carlo (MCMC) analysis with the combined Hubble and Pantheon datasets, conduct Om diagnostics, and construct $r-s$ plots to comment on the late behavior of our model. Through Om diagnostics, we find values located in phantom regions, as expected, owing to several physical reasons. Finally, we outline our future research directions.

**Keywords:** Chaplygin gas, scalar field, $f(Q)$ gravity, dark energy, Bose Einstein condensation, MCMC analysis, Om diagnostic, statefinder diagnostic

**DOI:** 10.1088/1674-1137/ae50e5 **CSTR:** 32044.14.ChinesePhysicsC.50065110

## I. INTRODUCTION

Since the discovery of late-time acceleration in the late 90s by Riess [1] and Perlmutter [2], it has been clear that Einstein's cosmological constant must be non-zero to explain late-time de Sitter type expansion. Moreover, studies of the galactic halo and structure formation, as well as baryonic acoustic oscillation (BAO) data, have revealed the existence of dark matter, which is weakly interacting, cold, and non-baryonic [3, 4]. Therefore, the period from the late 90s to the early 2000s was dominated by ΛCDM cosmology, in which dark energy (responsible for late time acceleration) is given by the cosmological constant (Λ) and dark matter (matter responsible for the galactic rotation curve anomaly) is cold and non-baryonic.

The standard model of cosmology, ΛCDM, is one of the most successful models and explains almost all present and past observations with only six free parameters. Although the ΛCDM paradigm is successful, there are still unanswered questions that raise doubts about standard cosmology. First, there is no way of explaining Λ in the standard cosmological model, even though identifying it with dark energy offers remarkable observational tests. For example, if one attempts to explain Λ (the cosmological constant) as simply vacuum energy, a serious problem occurs: a discrepancy on the order of $10^{120}$ is found between the observed value of Λ and the theoretical prediction obtained using one-loop corrections in QFT. To explain dark energy, one must use a scalar field (a quintessence field), which can explain the origin of Λ and why the cosmological constant is so small. There is an alternative method of explaining dark energy or late-time acceleration by modifying Einstein's theory of relativity. It is well known that standard general relativity (GR) is a classical theory and therefore breaks down in extreme-curvature regions, such as near singularities. To avoid this, one must quantize the theory, as in electromagnetism, to obtain a quantum theory of gravity. However, it is also well known that, despite numerous proposals, such as string theory and loop quantum gravity, a comprehensive theory of quantum

Received 9 December 2025; Accepted 12 March 2026; Accepted manuscript online 13 March 2026

* SG acknowledges the Council of Scientific and Industrial Research (CSIR), Government of India, New Delhi, for a senior research fellowship (File no.09/1026(13105)/2022-EMR-I). PKS acknowledges Anusandhan National Research Foundation (ANRF), Department of Science and Technology (DST), Government of India, for financial support to carry out Research project No.: CRG/2022/001847 and IUCAA, Pune, India, for providing support through the visiting associateship program

† E-mail: sayantanghosh.000@gmail.com
‡ E-mail: rajasolanki8268@gmail.com, raja.solanki@vitap.ac.in
§ E-mail: pksahoo@hyderabad.bits-pilani.ac.in

gravity (that can be experimentally or observationally tested) remains elusive [5, 6]. Athough we cannot find a full quantum gravity theory, we can make some reasonable guesses about how the Einstein-Hilbert action changes while maintaining diffeomorphism symmetry. Regarding CDM, the constituents of dark matter are not fully understood (in this study, we consider Chaplygin gas, which can explain both dark energy and dark matter in a unified framework of matter). Additionally, there is a growing concern in contemporary cosmology regarding Hubble ($H_0$) tension [7] and $\sigma_8$ [8]. Generally, these tensions indicate that our understanding of the full timescale of the universe is limited; that is, contemporary observations do not match those of the early and late universes, which challenges the current ΛCDM model profoundly.

One reason for such an anomaly is the importance of quantum effects in explaining the cosmological constant and dark matter. However, because no full quantum gravity theory exists, we can instead note the possible infrared behavior of quantum gravity theory. One loop correction of the graviton-graviton interaction can give rise to the $R^2$ term in the Einstein-Hilbert action, which has been used by Starobinsky [9] to predict inflation in the early universe. Therefore, modified gravity (MOG) is a lucrative alternative for explaining not only dark energy but also various other astrophysical phenomena (such as the super-Chandrasekhar mass limit [10] and black hole accretion [11]). The standard approach to modifying gravity is to modify the Einstein-Hilbert action with a suitable diffeomorphism-invariant scale and then derive the modified equation by varying the metric. Subsequently, a suitable metric (in this case, the Friedmann-Lemaitre-Robertson-Walker (FLRW) metric) can be inserted into the field equation to obtain the modified Einstein equations.

In this study, we consider $f(Q)$ gravity, a version of MOG based on non-metricity ($\nabla_\lambda g_{\mu\nu} \neq 0$) that reduces to GR in the linear limit. Although the actual origin of using non-metricity to unify electromagnetism and gravity dates back to the idea of Weyl, the modern version of $f(Q)$ cosmology was first proposed by Jimenez et al. [12] and later expanded by them [13, 14]. There are various papers that discuss the data analysis of cosmological models based on $f(Q)$ gravity in detail [15–20]. Moreover, there has been active effort to analytically study dark energy in the context of $f(Q)$ gravity via dynamical system analysis [21, 22]. Note that the $f(Q)$ MOG theory has shown remarkable consistency across various astrophysical objects, such as black holes [23], wormholes [24, 25], and gravastars [26, 27]. In this study, we consider Chaplygin gas as our matter source. Chaplygin gas has long been one of the most prominent candidates for dark energy. Section-II explains several reasons for this, such as the microscopical Chaplygin gas that arises naturally in string theory. The Chaplygin gas equation of state can also be naturally constructed using scalar and DBI fields, as well as brane compactification. On the phenomenological side, Chaplygin gas is not only consistent with current observations but can also provide a natural transition from matter to a dark-energy-dominated universe. Therefore, we use the most general equation of state for Chaplygin gas, which is given by $p = \alpha\rho + \beta\rho^m$.

Extensive studies have been conducted on the (non-gravitational) interaction between dark energy and dark matter over the past few decades. A standard quantum field theoretical approach is to consider the quintessence scalar field, whose effective mass becomes comparable to that of dark matter particles, to lead to an exchange of energy between the two components [28, 29]. There are several ways to model this interaction in the continuity equation, but the most simplistic and phenomenologically consistent method is via $\mathcal{I} \propto H\rho$. This encodes the FLRW geometry, which involves dilution via a factor of $H$ and is also consistent with the standard continuity equation. Such a model of the interaction between dark sectors has been widely used in the standard literature [30–32]. The interaction term relieves the tension between dark matter and dark energy, because an analysis with only Bose-Einstein condensation (BEC) dark matter yields $m = 2$, as investigated in detail in our previous study [33]. However, there is also an explicit dark energy component that is highly consistent with generalized Chaplygin gas, given as $m < 0$. Therefore, the presence of the interaction term provides a unified and physically motivated mechanism through which both branches emerge as viable solutions, with their relative relevance determined by observational constraints rather than imposed assumptions.

As previously mentioned, even though Chaplygin gas can effectively explain dark energy, it falls short in explaining dark matter. In this study, we consider dark matter as an effective Bose-Einstein condensate scalar field. There are two primary reasons for this, as explained in Section III. First, the Bose-Einstein condensate is a highly lucrative option for dark matter owing to its lack of viscosity, which may explain why galactic halos have uniform density. It is also visible from the microscopic perspective because the Gross-Pitaevskii equation for a moderately interacting dilute Bose gas can naturally provide an equation of state of the form $p = \alpha\rho + \beta\rho^2$, which is essentially Chaplygin gas with $m = 2$. Beyond the microscopic and phenomenological motivations, our study provides a unified framework that can be used to explain both dark energy and dark matter. We also include an interacting term, $\mathcal{I} = 3H^2\rho$, which facilitates a transition between dark matter and dark energy.

We perform Markov Chain Monte Carlo (MCMC) analysis using Hubble and Pantheon+ SH0ES data and test the model using two of the most popular statistical

tests: the AIC and BIC. We also perform the so-called null test for ΛCDM cosmology using statefinder and *Om* diagnostics.

## II. CHAPLYGIN GAS

Chaplygin gas was first proposed as a dark energy candidate by Kamenshchik *et al.* [34] with the relation $p \propto \rho^{-1}$, which can offer a smooth transition from matter-dominated ($\omega = 0$) to dark energy-dominated epochs ($\omega = -1$). This was later generalized by Bento et al. [35] with the relation $p \propto \rho^{-\alpha}$, where $\alpha$ is not necessarily one. Both the Chaplygin and generalized Chaplygin gas models provide remarkable constant solutions that explain the late-time acceleration and are consistent with observations. Even though Chaplygin gas has been mainly utilized as a candidate for dark energy, it appears naturally in quantum gravity theories, such as in the context of brane stabilization for AdS-Schwarzschild black holes to study the critical horizon [36] and in the study of 2+1 black holes in string theory [37]. Beyond string theory, there are other conventional methods of obtaining the Chaplygin equation of state, such as using the DBI field equation [38], scalar fields [39], or even the brane world scenario [36].

Chaplygin gas is a natural candidate for dark energy because it gives matter-dominated and dark-energy-dominated solutions and smoothly transitions between the two. However, detailed studies have shown that Chaplygin gas is not only a good candidate for phenomenology but is also extremely consistent with observational datasets. The review article in Ref. [40] provides a full analysis with an observational test. Consistency with dark energy using a Type IA supernova was reported [41, 42], and the consistency observed using CMB anisotropy data was also in favor of the Chaplygin gas theory [43]. Data on gravitational lensing [44], the age measurement of high-redshift objects [45], and the X-ray gas mass fraction of clusters [46] also suggest good agreement with the Chaplygin gas model as dark energy.

Here, we provide a short derivation of the scalar field, which can be responsible for Chaplygin gas under the influence of a scalar field (FLRW metric).

It is well known that the Lagrangian density of a scalar field can be written as

$$\mathcal{L}(\phi) = -\frac{1}{2} g^{\mu\nu}\partial_\mu\phi\partial_\nu\phi - V(\phi). \tag{1}$$

The stress-energy tensor is given by

$$T^{\phi}_{\mu\nu} = \partial_\mu\phi\partial_\nu\phi - \frac{1}{2} g_{\mu\nu} g_{\alpha\beta}\partial^\alpha\phi\partial^\beta\phi - g_{\mu\nu}V(\phi). \tag{2}$$

Moreover, the variation in the Lagrangian with respect to $\phi$ gives the Klein-Gordon equation

$$\Box\phi - V_{,\phi}(\phi) = 0, \tag{3}$$

where $V_{,\phi} = \dfrac{\partial V}{\partial\phi}$.

Calculating the stress-energy tensor ($T_{\mu\nu}$) with such a Lagrangian and equating it with $\rho_\phi$ and $p_\phi$ as a fluid analog results in an expression for density and pressure on an FLRW background with the metric $\mathrm{d}s^2 = \mathrm{d}t^2 - a^2(t)\mathrm{d}l^2$, where $\mathrm{d}l^2$ is a typical spherically symmetric line element. Then, we can obtain the expressions for $\rho_\phi$ and $p_\phi$ as follows:

$$\rho_\phi = \frac{1}{2}\dot{\phi}^2 + V(\phi) = \sqrt{A + \frac{B}{a^6}}, \tag{4}$$

and

$$p_\phi = \frac{1}{2}\dot{\phi}^2 - V(\phi) = -\frac{A}{\sqrt{A + \dfrac{B}{a^6}}}. \tag{5}$$

From Eqs. (4) and (5), we get

$$\dot{\phi}^2 = \frac{B}{a^6\sqrt{A + \dfrac{B}{a^6}}}, \tag{6}$$

and

$$V(\phi) = \frac{2a^6\left(A + \dfrac{B}{a^6}\right) - B}{2a^6\sqrt{A + \dfrac{B}{a^6}}}. \tag{7}$$

Taking the derivative with respect to $a$ gives

$$\phi' = \frac{\sqrt{B}}{a(Aa^6 + B)^{\frac{1}{2}}}, \tag{8}$$

where " $'$ " denotes the derivative with respect to $a$.

The above expression can be integrated to obtain

$$a^6 = \frac{4B\exp(6\phi)}{A(1 - \exp(6\phi))^2}. \tag{9}$$

Substituting this into Eq. (7) provides an expression for $V(\phi)$ as follows:

$$V(\phi) = \frac{1}{2}\sqrt{A}\left(\cosh 3\phi + \frac{1}{\cosh 3\phi}\right). \tag{10}$$

As shown above, a potential scalar field is given by $V(\phi)=\frac{1}{2}\sqrt{A}\left(\cosh 3\phi+\frac{1}{\cosh 3\phi}\right)$ (where $B$ is an integration constant obtained by solving the Friedmann equation).

Now, we consider a method of recovering the Chaplygin gas equation of state from tachyons.

First, tachyon-based action or DBI field action can be written as

$$\mathcal{S}=-\int \mathrm{d}^4x\sqrt{-g}V(T)\sqrt{1-g^{\mu\nu}T_{,\mu}T_{,\nu}}. \tag{11}$$

We express the Lagrangian density as follows:

$$L=-V(T)\sqrt{1-\dot{T}^2}. \tag{12}$$

Here, we define $T=g^{\mu\nu}T_{,\mu}T_{,\nu}$ as the kinetic term of the Lagrangian.

As in the previous case, if the stress energy tensor ($T_{\mu\nu}$) is calculated and equated with the fluid stress energy tensor, the following expressions for $\rho_{Tac}$ and $p_{Tac}$ can be obtained:

$$\rho_{Tac}=\frac{V(T)}{\sqrt{1-\dot{T}^2}}, \tag{13}$$

and

$$p_{Tac}=-V(T)\sqrt{1-\dot{T}^2}. \tag{14}$$

Using the previous expressions for $\rho_{Tac},p_{Tac}$ with the Friedmann equations, the potential can be derived as [39]

$$V(T)=\frac{\Lambda}{\sin^2\left(\frac{3\sqrt{\Lambda(1+k)}T}{2}\right)}\left(\sqrt{1-(1+k)\cos^2\left(\frac{3\sqrt{\Lambda(1+k)}T}{2}\right)}\right). \tag{15}$$

Additionally, the kinetic energy term is given by

$$T(t)=\frac{2}{3\sqrt{\lambda(1+k)}}\operatorname{arctan\,sinh}\frac{3\sqrt{\Lambda}(1+k)t}{2}. \tag{16}$$

Now, we address the generalized Chaplygin gas equation of state and show that such an equation can also be produced via a scalar field in an FLRW background.

Note that the general equation of state for generalized Chaplygin gas is given as follows:

$$p=A\rho-\frac{B}{\rho^{\chi}}. \tag{17}$$

If we take the stress-energy tensor and equate it with fluid, the following expression for $U(\varphi)$ can be obtained [39]:

$$U(\varphi)=\frac{1}{2}\left(\frac{B}{A+1}\right)^{\frac{1}{\chi+1}}\left[\frac{1+A}{\cosh^{\frac{2\chi}{\chi+1}}\left(\varpi(\chi+1)\Delta\varphi\right)}+(1-A)\cosh^{\frac{2}{\chi+1}}\left(\varpi(\chi+1)\Delta\varphi\right)\right]. \tag{18}$$

Here, $\Delta\varphi=\varphi-\varphi_0$ (where $\varphi_0$ is an integration constant), and $\varpi=\sqrt{\frac{(D-1)(A+1)}{2(D-2)}}$ (in our case, $D=4$). Similarly, the generalized [39] Chaplygin gas equation of state can be found via the tachyon field.

Using the Randall-Sundrum model [47], where a dimension is wrapped, the metric can be written as

$$\mathrm{d}s^2=\mathrm{e}^{\frac{-2|y|}{l}}(\mathrm{d}t^2-\mathrm{d}x_1{}^2-\mathrm{d}x_2{}^2-\mathrm{d}x_3{}^2)-\mathrm{d}y^2, \tag{19}$$

where $y$ is the coordinate for the extra dimension, and $l$ is often called the "wrapping factor." At $y=0$, there is a singularity (the derivative is discontinuous), which implies a brane-like object embedded in the fifth dimension.

For such a metric, the following equation of state can be obtained [36]:

$$p=\frac{-(n-1)\rho}{n}-\frac{4n}{\rho l^2}. \tag{20}$$

Here, $n$ denotes the dimension of branes. We assume that the manifold (orbifold) has a local $R\times S^n$ topology (Chaplygin gas-dominated anisotropic brane world cosmological models).

As shown, the Randall-Sundrum model naturally gives rise to the generalized Chaplygin gas equations.

Note that, for the remainder of our manuscript, we express the Chaplygin gas equation of state as

$$p=\alpha\rho+\beta\rho^m. \tag{21}$$

Here, we use $A,B,\chi$ for consistency with the literature (for example, $\chi^2$ and Models A and B); consequently, we take the equation of state to be $p=\alpha\rho+\beta\rho^m$. Moreover, the purpose of this section is to show that the Chaplygin gas equation of state cannot be obtained from only a scalar field. Instead, Eqs. (13) or (16) can be reversed to reconstruct the appropriate scalar field potential or DBI field potential from the known parameters of the Chaplygin gas equation.

## III. DARK MATTER FROM THE BEC

BEC is an effect of Bose-Einstein statistics predicted

by Einstein. Because boson wave functions are symmetric under interchange, there is a possibility of significant degeneracy at the lowest temperature, which could give rise to condensation at very low temperatures. It was first experimentally verified by Bradley *et al*. [48]. Athough BEC is an important concept in condensed matter physics as it provides a partial explanation for superfluidity and superconductivity, it can also be used as an effective theory for dark matter owing its noninteractive nature.

Although many studies have conjectured the Bose-Einstein condensate to be a dark-matter candidate, it was Boehmer and Harko [49] who provided a solid reason why this theory should be taken seriously. Because the critical temperature for BEC to occur is close to that of the interstellar medium, the scalar fields responsible for dark matter may also condense. This could naturally explain the uniformity of the dark matter halo observed at the galactic center. Harko [50] later expanded this idea, noting how the temperature dependence of the early universe could cause the scalar field to condense to a Bose-Einstein condensate. Their paper also discussed how the scalar field satisfying the Gross-Pitaevskii equation for a weakly interacting Bose gas could give rise to superfluidity and, in principle, explain the uniform density of the galactic halo. In a later study by Harko and Lobo [51], the analysis was extended to include gravitational lensing, which was shown to be remarkably consistent with current observations.

A similar type of treatment can be performed for other dark energy models, such as dark matter using a Lagrangian with global symmetry [52], an extra dimension (brane world) responsible for dark matter [53], and a primordial black hole as a candidate for dark matter [54]. Axion dark matter [55] also gives a similar equation of state after condensation. Das et al. [56, 57] showed that the quantum potential can be used to obtain a similar equation of state.

Finally, the BEC equation of state was used by Mahichi et al. [58−60] in various MOG scenarios, such as $f(T,B)$ and Gauss-Bonnet gravity.

Here, we briefly outline a method of addressing weakly interacting gravitationally bound boson particles, as discussed by Harko [50]. One key note is that BEC occurs at very low temperatures and when quantum effects are significant. More precisely, weakly interacting particles undergo BEC provided that this condition is satisfied, that is, $T_{\rm cr} \approx 2\pi \times \hbar^2 \rho^{2/3}/m^{5/3}k_B$. Such conditions are physically possible during the structural formation time in cosmology. Now, to include the weak interactions between bosons, the potential form is taken as $V(r'-r) = \lambda\delta(r'-r)$, where $\lambda$ is a dimensionally consistent length scale associated with the interaction. The functional energy ($\mathcal{E}$) for such weakly interacting bosons can be expressed by the Gross-Pitaevskii formula:

$$\mathcal{E}[\psi] = \int \left[\frac{\hbar^2}{2m_\chi}|\nabla\psi(\vec{r})|^2 + \frac{U_0}{2}|\psi(\vec{r})|^4\right] \mathrm{d}\vec{r} - \frac{1}{2}Gm_\chi^2 \int\int \frac{|\psi(\vec{r})|^2|\psi(\vec{r}')|^2}{|\vec{r}-\vec{r}'|}\mathrm{d}\vec{r}\mathrm{d}\vec{r}' . \quad (22)$$

Here, $\psi$ is analogous to the entire wave function for the many-body system. Therefore, following this, the mass density can be defined as

$$\rho_\chi(\vec{r}) = m_\chi|\psi(\vec{r})|^2 = m_\chi\rho(\vec{r}). \quad (23)$$

Additionally, the total number of dark matter particles can be given as $N = \int |\psi(\vec{r})|^2 \mathrm{d}^3x$. From the above energy functional, the variational principle can be used to reach the Schrodinger-like equation for $\psi$ for weakly interacting Bose particles under gravitational attraction:

$$-\frac{\hbar^2}{2m_\chi}\nabla^2\psi(\vec{r}) + m_\chi V(\vec{r})\psi(\vec{r}) + U_0|\psi(\vec{r})|^2\psi(\vec{r}) = \mu\psi(\vec{r}). \quad (24)$$

Finally, to obtain the desired equation of state, a trial wave function must be chosen in the plane polar coordinate, $\psi(\vec{r},t) = \sqrt{\rho(\vec{r},t)}\exp\left[\frac{\mathrm{i}}{\hbar}S(\vec{r},t)\right]$, similar to the Grizberg-Landau ansatz to obtain the uncertainty relation in the phase or chemical potential.

In this analysis, we consider dark matter as a bosonic substance whose number density follows Bose-Einstein statistics. This statistical behavior suggests that such particles emerged from the thermal decoupling of early-universe plasma. The energy density of standard bosonic dark matter is defined by the product of its number density and particle mass. Its pressure, according to Bose-Einstein statistics, can be described within a sphere defined by the momentum radius of the particles. Under these assumptions, the pressure of normal dark matter is found to vary linearly with the energy density, leading to the equation of state:

$$p = \alpha\rho, \quad (25)$$

where $\alpha$ denotes the proportionality constant associated with single-body interactions in the dark-matter medium.

We now extend this description to a Bose-Einstein condensate form of dark matter, comprising non-relativistic bosons undergoing two-body interactions at extremely low temperatures. As the temperature approaches absolute zero, quantum effects become dominant, and individual particle wave functions overlap, resulting in condensation into a single quantum state. The dynamics of such a condensate are governed by the Gross-Pitaevskii equation. Within a gravitational context, the pressure of BEC dark matter is shown to follow a

quadratic dependence on energy density:

$$p = \beta\rho^2, \tag{26}$$

where $\beta$ encapsulates the interaction strength through the mass of the particles and the length of the scattering. To incorporate both conventional and BEC-like behaviors, an extended form of the dark matter equation of state, referred to as the extended Bose-Einstein condensate, is proposed:

$$p = \alpha\rho + \beta\rho^2. \tag{27}$$

Here, the linear term $\alpha\rho$ accounts for single-particle effects, whereas the nonlinear term $\beta\rho^2$ reflects two-body interactions. Special cases of this model recover various dark matter scenarios: $\alpha = \beta = 0$ corresponds to cold dark matter, $\beta = 0$ recovers normal dark matter, and $\alpha = 0$ isolates the BEC contribution from dark matter halos.

## IV. UNIFORM FRAMEWORK FOR DARK ENERGY AND DARK MATTER

In this study, we employ the generalized Chaplygin gas model to describe both dark energy and dark matter using a single equation of state, given as $p = \alpha\rho + \beta\rho^m$. As discussed in previous sections, "pure" Chaplygin gas can be obtained for $m < 0$, which is responsible for dark energy, and for $m = 2$, we obtain $p = \alpha\rho + \beta\rho^2$, which is simply the equation of state of BEC dark matter. At this point, we bifurcate the models. In one model, we obtain $m \approx -5$, which is consistent with the Chaplygin gas model as dark energy. However, we also get $m \approx 2$ for another set of MCMCs with different priors. This is highly consistent with being a BEC dark matter equation of state. With this in mind, we must add an interaction term between dark matter and dark energy, such as $\mathcal{I}$, which will address the positive energy transfer from dark matter to dark energy when $\mathcal{I} > 0$, and vice versa for $\mathcal{I} < 0$. To fix a form of $\mathcal{I}$, the dimensional analysis suggests a natural form in terms of $[\rho][T^{-1}]$; hence, the most obvious choice is $\mathcal{I} \propto \rho H$. Therefore, following convention, we take the proportional constant to be $3b^2$ ($b^2$ to ensure the expression is positive). Note that there are alternatives for the interaction term, as discussed in Refs. [61−63].

## V. FORMULATION OF $f(Q)$ GRAVITY

Athough Einstein used the Levi-Civita connection to construct the field equation in the original formulation of GR, it was soon clear that one can (uniquely) split the most general connection on a tangent bundle over a manifold into three different parts: Levi-Civita, anti-symmetric, and non-metricity. The proof and motivation for this can be found in a review article by Heisenberg [64]. Therefore, in principle, the most general affine connection can be written in the form [14]

$$\Upsilon^{\alpha}_{\ \mu\nu} = \Gamma^{\alpha}_{\ \mu\nu} + K^{\alpha}_{\ \mu\nu} + L^{\alpha}_{\ \mu\nu}. \tag{28}$$

Here, the first term $\Gamma^{\alpha}_{\ \mu\nu}$ denotes the usual Levi-Civita connection

$$\Gamma^{\alpha}_{\ \mu\nu} \equiv \frac{1}{2} g^{\alpha\lambda}(g_{\mu\lambda,\nu} + g_{\lambda\nu,\mu} - g_{\mu\nu,\lambda}). \tag{29}$$

The second term $K^{\alpha}_{\ \mu\nu}$ is known as the contortion tensor. The formula can be expressed in the form of a torsion tensor ($T^{\alpha}_{\ \mu\nu} \equiv \Upsilon^{\alpha}_{\ \mu\nu} - \Upsilon^{\alpha}_{\ \nu\mu}$) as follows:

$$K^{\alpha}_{\ \mu\nu} \equiv \frac{1}{2}(T^{\alpha}_{\ \mu\nu} + T_{\mu\ \nu}^{\ \alpha} + T_{\nu\ \mu}^{\ \alpha}). \tag{30}$$

Finally, the last term is known as the distortion tensor, which is the most relevant to our study. The formula given in the form of the non-metricity tensor is

$$L^{\alpha}_{\ \mu\nu} \equiv \frac{1}{2}(Q^{\alpha}_{\ \mu\nu} - Q_{\mu\ \nu}^{\ \alpha} - Q_{\nu\ \mu}^{\ \alpha}). \tag{31}$$

The expression for the non-metricity tensor is given as

$$Q_{\alpha\mu\nu} \equiv \nabla_{\alpha} g_{\mu\nu} = \partial_{\alpha} g_{\mu\nu} - \Upsilon^{\beta}_{\ \alpha\mu} g_{\beta\nu} - \Upsilon^{\beta}_{\ \alpha\nu} g_{\mu\beta}. \tag{32}$$

We can also define the superpotential tensor as follows:

$$4P^{\lambda}_{\ \mu\nu} = -Q^{\lambda}_{\ \mu\nu} + 2Q_{(\mu\ \ \nu)}^{\ \ \lambda} + (Q^{\lambda} - \tilde{Q}^{\lambda}) g_{\mu\nu} - \delta^{\lambda}_{(\mu} Q_{\nu)}, \tag{33}$$

where $Q_{\alpha} = Q_{\alpha\ \mu}^{\ \mu}$ and $\tilde{Q}_{\alpha} = Q^{\mu}_{\ \alpha\mu}$ are non-metricity vectors. If the non-metricity tensor is contracted with the superpotential tensor, the non-metricity scalar ($Q$) can be obtained as follows:

$$Q = -Q_{\lambda\mu\nu} P^{\lambda\mu\nu}. \tag{34}$$

The Riemann curvature tensor is given as follows:

$$R^{\alpha}_{\ \beta\mu\nu} = 2\partial_{[\mu} \Upsilon^{\alpha}_{\ \nu]\beta} + 2\Upsilon^{\alpha}_{\ [\mu|\lambda|} \Upsilon^{\lambda}_{\ \nu]\beta}. \tag{35}$$

Now, using the affine connection (24), we have

$$R^{\alpha}_{\ \beta\mu\nu} = \mathring{R}^{\alpha}_{\ \beta\mu\nu} + \mathring{\nabla}_{\mu} X^{\alpha}_{\ \nu\beta} - \mathring{\nabla}_{\nu} X^{\alpha}_{\ \mu\beta} + X^{\alpha}_{\ \mu\rho} X^{\rho}_{\ \nu\beta} - X^{\alpha}_{\ \nu\rho} X^{\rho}_{\ \mu\beta}. \tag{36}$$

Here, $\mathring{R}^{\alpha}_{\beta\mu\nu}$ and $\mathring{\nabla}$ are described in terms of the Levi-Civita connection (25). Note that $X^{\alpha}_{\mu\nu} = K^{\alpha}_{\mu\nu} + L^{\alpha}_{\mu\nu}$. If we use the contraction on the Riemann curvature tensor with the torsion-free constraint $T^{\alpha}_{\mu\nu} = 0$ in Eq. (32), we obtain the following:

$$R = \mathring{R} - Q + \mathring{\nabla}_{\alpha}\left(Q^{\alpha} - \tilde{Q}^{\alpha}\right). \tag{37}$$

Here, $\mathring{R}$ is the typical Ricci scalar evaluated with respect to the Levi-Civita connection. We also use the teleparallel constraint (the choice of such a gauge is explained in detail in Ref. [64]), *i.e.*, $R = 0$. Using the teleparallel constraint, Eq. (33) becomes

$$\mathring{R} = Q - \mathring{\nabla}_{\alpha}\left(Q^{\alpha} - \tilde{Q}^{\alpha}\right). \tag{38}$$

Eq. (34) shows that the Ricci scalar (using the Levi-Civita connection) differs from the non-metricity scalar ($Q$) by a total derivative. Using a generalized Stokes theorem, this total derivative can be transformed into a boundary term. Therefore, the Lagrangian density changes by a boundary term, and as far as the action is concerned, $Q$ is equivalent to $\mathring{R}$. $Q$ gives a comparable description of GR with curvature. Moreover, because we take the torsion to be zero, the theory is known as a symmetric teleparallel equivalent to GR (STEGR) [65].

A general form of STEGR theory in the presence of matter using a general form of $f(Q)$ in the action is expressed as follows:

$$\mathcal{S} = \int \frac{1}{2} f(Q)\sqrt{-g}\,\mathrm{d}^4x + \int \mathcal{L}_m\sqrt{-g}\,\mathrm{d}^4x, \tag{39}$$

where $g = \det(g_{\mu\nu})$, and $f(Q)$ is a function of the non-metricity scalar $Q$.

## VI. COSMOLOGY IN $f(Q)$ GRAVITY

A study [66] showed that, for the homogeneous and isotropic Riemannian manifold, the FLRW metric is a unique metric up to diffeomorphism. As of now, from the large-scale galaxy survey [67] and latest CMB dataset from Planck [68], our universe is considered to be not only homogeneous and isotropic but also flat to a high degree. Therefore, in this study, we only consider the flat FLRW metric in our calculations, which is given by

$$\mathrm{d}s^2 = -\mathrm{d}t^2 + a^2(t)[\mathrm{d}x^2 + \mathrm{d}y^2 + \mathrm{d}z^2]. \tag{40}$$

Here, $a(t)$ is the scale factor of the expanding universe.

For the teleparallel consideration, we use the constraint corresponding to the flat geometry of a pure inertial connection. We use a gauge transformation given by $\Lambda^{\alpha}_{\mu}$ [13] to obtain the following form:

$$\Upsilon^{\alpha}_{\mu\nu} = (\Lambda^{-1})^{\alpha}_{\beta}\partial_{[\mu}\Lambda^{\beta}_{\nu]}. \tag{41}$$

We can also express the general affine connection by noting that a general element of the group $GL(4,\mathbb{R})$ is characterized by the transformation $\Lambda^{\alpha}_{\mu} = \partial_{\mu}\zeta^{\alpha}$, where $\zeta^{\alpha}$ is an arbitrary vector field,

$$\Upsilon^{\alpha}_{\mu\nu} = \frac{\partial x^{\alpha}}{\partial\zeta^{\rho}}\partial_{\mu}\partial_{\nu}\zeta^{\rho}. \tag{42}$$

Owing to gauge redundancy, the connection (38) can be eliminated by choosing an appropriate coordinate transformation. Such a coordinate transformation is often known as a "gauge coincidence." Using the coincident gauge, the non-metricity scalar corresponding to the metric (36) becomes $Q = 6H^2$.

The energy-momentum tensor for a perfect fluid distribution is given as follows:

$$T_{\mu\nu} = (\rho + p)u_{\mu}u_{\nu} + pg_{\mu\nu}, \tag{43}$$

where we take $u_{\mu} = (-1,0,0,0)$ as components of the four velocities, which is consistent with the signature of the metric.

From the field equation in the FLRW background, in the presence of a matter field, the following Friedmann-like equations can be obtained:

$$3H^2 = \frac{1}{2f_Q}\left(-\rho + \frac{f}{2}\right), \tag{44}$$

$$\dot{H} + 3H^2 + \frac{\dot{f}_Q}{f_Q}H = \frac{1}{2f_Q}\left(p + \frac{f}{2}\right). \tag{45}$$

## VII. COSMOLOGY WITH CHAPLYGIN GAS IN $f(Q)$ GRAVITY

Eqs. (40) and (41), along with the symmetric teleparallel field equation under the FLRW metric, can be decoupled to form a dark energy term.

Therefore, Eqs. (40) and (41) can be rewritten as follows:

$$3H^2 = \rho + \rho_{\mathrm{de}}, \tag{46}$$

$$\dot{H} = -\frac{1}{2}[\rho + p + \rho_{\mathrm{de}} + p_{\mathrm{de}}], \tag{47}$$

and $\rho_{de}$ and $p_{de}$ become

$$\rho_{de} = \frac{1}{2}(Q - f) + Qf_Q, \tag{48}$$

$$p_{de} = -\rho_{de} - 2\dot{H}(1 + f_Q + 2Qf_{QQ}). \tag{49}$$

Note that, by using the above equations, it immediately follows that

$$\dot{\rho}_{de} + 3H(\rho_{de} + p_{de}) = 0. \tag{50}$$

The geometric dark energy components $\rho_{de}$ and $p_{de}$ resulting from $f(Q)$ geometry satisfy the conservation identity (46). For phenomenological purposes, we can introduce an effective interacting dark energy fluid through a non-unique splitting of the total energy-momentum tensor as follows:

$$\dot{\rho}^{\rm eff}_{de} + 3H(\rho^{\rm eff}_{de} + p^{\rm eff}_{de}) = \mathcal{I} \tag{51}$$

and

$$\dot{\rho} + 3H(\rho + p) = -\mathcal{I}, \tag{52}$$

where $\rho^{\rm eff}_{de} = \rho_{de} + \rho_{\rm int}$, $p^{\rm eff}_{de} = p_{de} + p_{\rm int}$, and $\mathcal{I} = 3b^2H\rho$ [61−63]. Here, $\rho_{de}$ and $p_{de}$ are the quantities arising from $f(Q)$ geometry, and $\rho_{\rm int}$ and $p_{\rm int}$ account for the energy exchange arising from the interaction of dark energy and dark matter. In this framework, the effective dark energy originates from the contributions of both the geometric sector through the $f(Q)$ gravity function and the generalized Chaplygin gas matter sector. Therefore, the late-time acceleration in our model is not solely geometric in origin but results from a combined contribution of MOG and the exotic matter sector. The interaction term further couples these two effective components, leading to richer cosmological dynamics. Moreover, note that the continuity equation holds as a full set of $\rho$ and $p$ as follows:

$$(\dot{\rho} + \dot{\rho}^{\rm eff}_{de}) + 3H(\rho + p + \rho^{\rm eff}_{de} + p^{\rm eff}_{de}) = 0. \tag{53}$$

We take the form of $f(Q)$ as a monomial, that is,

$$f(Q) = \gamma\left(\frac{Q}{Q_0}\right)^n, \tag{54}$$

and we obtain the following from the first Friedmann equation:

$$\rho = \frac{1-2n}{2}\gamma\left(\frac{H}{H_0}\right)^{2n}. \tag{55}$$

Taking $\rho_0$ as the present $\rho$, we get

$$\rho = \rho_0\left(\frac{H}{H_0}\right)^{2n}. \tag{56}$$

Now, taking the generalized Chaplygin gas and integrating the continuity (Eq. (48)), the density can be obtained as

$$\rho = \rho_0\left(\frac{c\eta a_0^{3\eta(m-1)} - \beta}{c\eta a^{3\eta(m-1)} - \beta}\right)^{\frac{1}{(m-1)}}. \tag{57}$$

Consequently, the scale factor is

$$H = H_0\left(\frac{c\eta a_0^{3\eta(m-1)} - \beta}{c\eta a^{3\eta(m-1)} - \beta}\right)^{\frac{1}{2n(m-1)}}. \tag{58}$$

## VIII. STATISTICAL ANALYSIS AND DATASETS

In this section, we compare the predictions of the theoretical model with observational data to constrain the free parameters. We use a joint sample consisting of 31 cosmic chronometer (CC) measurements and the Pantheon+SH0ES compilation of 1701 Type Ia supernovae. Bayesian statistical methods are employed, using a likelihood-based approach and MCMC sampling, to estimate the posterior distributions of the parameters.

### A. Cosmic Chronometers (CC)

CCs are massive, passively evolving galaxies whose star formations have ceased [69]. The age differences of these galaxies at nearby redshifts provide a direct estimate of the Hubble parameter $H(z)$ via

$$H(z) = -\frac{1}{1+z}\frac{{\rm d}z}{{\rm d}t}. \tag{59}$$

In this study, we use 31 independent $H(z)$ measurements in the range $0.07 \le z \le 2.41$ [70, 71]. For each measurement $k$, with observed value $H_{{\rm obs},k}$, uncertainty $\sigma_{H,k}$, and model prediction $H_{\rm th}(z_k)$, the chi-squared value is

$$\chi^2_{\rm CC} = \sum_{k=1}^{31}\frac{\left[H_{\rm th}(z_k) - H_{{\rm obs},k}\right]^2}{\sigma^2_{H,k}}. \tag{60}$$

### B. Pantheon+SH0ES Supernovae (SN)

The Pantheon+SH0ES compilation contains 1701 Type Ia supernovae that span redshifts of $0.001 \le z \le 2.3$.

These supernovae act as standardizable candles via the distance modulus

$$\mu^{\rm th}(z) = 5\log_{10}\left(\frac{D_L(z)}{\rm Mpc}\right) + 25, \tag{61}$$

where the luminosity distance is

$$D_L(z) = c(1+z)\int_0^z \frac{{\rm d}x}{H(x,\theta)}. \tag{62}$$

During the past two decades, several Type Ia supernova compilations have been developed, beginning with the Union sample [72], followed by the Union2 [73], Union2.1 [74], JLA compilation [75], Pantheon [76], and, most recently, the Pantheon+SH0ES dataset [77].

For each supernova with observed peak magnitude $m_{B,i}$ and absolute magnitude $M$, the residual vector is

$$D_i = m_{B,i} - M - \mu^{\rm th}(z_i). \tag{63}$$

To break the $M$–$H_0$ degeneracy, Pantheon+SH0ES replaces $\mu^{\rm th}$ with Cepheid-calibrated distances $\mu_i^{\rm Ceph}$ for host galaxies with independent calibrations:

$$\bar{D}_i = \begin{cases} m_{B,i} - M - \mu_i^{\rm Ceph}, & \text{Cepheid hosts,} \\ m_{B,i} - M - \mu^{\rm th}(z_i), & \text{otherwise.} \end{cases} \tag{64}$$

With the covariance matrix $C_{\rm SN}$ (including systematics), the supernova chi-squared value is

$$\chi^2_{\rm SN} = \bar{\mathbf{D}}^{\rm T} C_{\rm SN}^{-1} \bar{\mathbf{D}}. \tag{65}$$

### C. Joint Likelihood

The combined chi-squared value minimized in the MCMC analysis is

$$\chi^2_{\rm total} = \chi^2_{\rm CC} + \chi^2_{\rm SN}. \tag{66}$$

### D. Results and Constraints

From the combined CC+Pantheon+SH0ES dataset, the best-fit parameters with 68% confidence limits for the Chaplygin gas model (Model-I) are as follows:

The minimum chi-squared value for the fit is

$$\chi^2_{\rm min} = 1644.828. \tag{67}$$

**Table 1.** Best-fit cosmological parameters with 68% confidence intervals.

| Parameter | Gaussian Priors | Best fit $\pm1\sigma$ |
|---|---|---|
| $H_0$ | $72.14 \pm 1.0$ | $73^{+0.19}_{-0.18}$ |
| $n$ | $0.014 \pm 0.1$ | $0.52^{+0.03}_{-0.03}$ |
| $\beta$ | $2.3 \pm 0.2$ | $0.86^{+0.1}_{-0.1}$ |
| $\eta$ | $0.22 \pm 0.2$ | $0.45^{+0.02}_{-0.021}$ |
| $c$ | $-0.31 \pm 0.1$ | $-0.62^{+0.046}_{-0.046}$ |
| $m$ | $-0.49 \pm 0.2$ | $-5^{+0.098}_{-0.098}$ |
| $\chi^2_{\rm min}$ | | 1644.828 |

For BEC ($m \approx 2$) (Model-II), the best-fit values are given as

The minimum chi-squared value for the fit is

$$\chi^2_{\rm min} = 1634.029. \tag{68}$$

Tables 1 and 2 list the Gaussian priors for the Model-I and Model-II respectively.

### E. Model Comparison via the AIC and BIC

The Akaike information criterion (AIC) [78] measures relative predictive accuracy while penalizing model complexity, whereas the Bayesian information criterion (BIC) [79] approximates Bayesian model evidence, with a stronger penalty for additional parameters as the sample size increases. In this study, both criteria are computed from $\chi^2$ fits, and models are compared based on differences with respect to the minimum-IC model, following standard $\Delta$ thresholds.

Athough the AIC and BIC are commonly used in general Bayesian analysis, they were first systematically introduced in the context of cosmology by Liddle [80]. The AIC is defined as

$$\text{AIC} = \chi^2_{\rm min} + 2d, \tag{69}$$

where $d$ is the number of free parameters in the model. To compare our results with those of the standard $\Lambda$CDM model, we compute the difference

$$\Delta\text{AIC} = |\text{AIC}_{\rm MOG} - \text{AIC}_{\Lambda\rm CDM}|. \tag{70}$$

A value of $\Delta\text{AIC} < 2$ indicates strong support for the MOG model, whereas $4 < \Delta\text{AIC} \leq 7$ suggests moderate evidence. If $\Delta\text{AIC} > 10$, there is no significant support for the MOG model.

The BIC is defined as

**Table 2.** Best-fit cosmological parameters with 68% confidence intervals.

| Parameter | Gaussian Priors | Best fit $\pm1\sigma$ |
|---|---|---|
| $H_0$ | $72.09\pm1.0$ | $73^{+0.19}_{-0.2}$ |
| $n$ | $-0.064\pm0.1$ | $-2^{+0.005}_{-0.0049}$ |
| $\beta$ | $0.05\pm0.2$ | $0.51^{+0.0047}_{-0.0045}$ |
| $\eta$ | $-1.5\pm0.2$ | $-1.7^{+0.042}_{-0.042}$ |
| $c$ | $-0.0006\pm0.1$ | $-0.019^{+0.0024}_{-0.0022}$ |
| $m$ | $1.22\pm0.2$ | $1.8^{+0.051}_{-0.052}$ |
| $\chi^2_{\rm min}$ | | 1634.029 |

$$\mathrm{BIC} = \chi^2_{\rm min} + d\ln(N), \tag{71}$$

where $N$ is the number of data points used in the MCMC analysis. The interpretation is similar:

- $\Delta\mathrm{BIC} < 2$: strong support for MOG,
- $2 \le \Delta\mathrm{BIC} < 6$: moderate support,
- $\Delta\mathrm{BIC} > 6$: weak or no support.

The computed AIC and BIC values for the viscous MOG models considered are summarized in Table 3. Based on these results, there is strong evidence in favor of the proposed models across all three datasets. In particular, Model I demonstrates the closest agreement with the ΛCDM model.

## IX. OM DIAGNOSTICS AND STATE FINDER ANALYSIS

Several tests have been proposed to assess deviations from the ΛCDM model, known as null tests for standard cosmological models. The concept involves constructing a scalar quantity (real numbers) that gives a particular value for ΛCDM and only deviates when the model is not ΛCDM. Ideally, these quantities should also distinguish between two different types of nonstandard cosmologies, such as quintessence and phantoms.

In this study, we primarily use two diagnoses, Om and statefinder diagnoses, to test the deviation from ΛCDM. Although the MCMC analysis shows the best fit model parameters with the latest observational data, such as the Hubble and Pantheon+SH0ES datasets, the late-time behavior of our model remains unclear, that is, whether it approaches the de-Sitter model from the phantom or quintessence side. These diagnoses provide a good consistency check to acertain whether the results are late-time de Sitter solutions and understand the severity of the deviation from those of ΛCDM.

### A. Om Diagnostics

Om diagnostics is the simplest form of diagnosis available for the classification of various dark energy-based cosmological models and their deviation from ΛCDM.

It was first proposed by Sahni *et al*. [81], who noted that the matter density falls as a third power of the scalar factor while Λ remains constant. The formula for $Om(z)$ is given as

$$Om(z) = \frac{\left(\frac{H(z)}{H_0}\right)^2 - 1}{(1+z)^3 - 1}. \tag{72}$$

In our study, we plot this relationship and find that, for approximately $z > 1$, the slope is negative, indicating the quintessence scenario, whereas for $-1 < z < 1$, the slope is positive, indicating the phantom scenario. Therefore, for both of our cases (the Chaplygin gas ($m \approx -5$) and BEC ($m \approx 2$), the quintessence scenario is observed up to $z = 1$, and then, from $z = 1$ to the present ($z = 0$) and future ($z < 0$), the phantom behavior occurs to reach the de Sitter solution or ΛCDM. Therefore, both of our models exhibit late-time phantom-like behavior. This is not a contradiction, as the $Om$ is susceptible to full integration rather than the local instantaneous $\omega$. In a sense, it meas-

**Table 3.** Minimum $\chi^2$ values and the corresponding AIC and BIC values for both Chaplygin gas (Model-1) and BEC dark matter (Model-2)

| Model | Dataset | $\chi^2_{\rm min}$ | | AIC | | BIC | | ΔAIC | ΔBIC |
|---|---|---|---|---|---|---|---|---|---|
| | | MOG | ΛCDM | MOG | ΛCDM | MOG | ΛCDM | | |
| I | CC | 28.001 | 32.132 | 40.001 | 38.132 | 48.604 | 42.431 | 1.869 | 6.173 |
| | Pantheon+ | 1616.827 | 1609.917 | 1628.827 | 1615.917 | 1661.460 | 1632.231 | 12.91 | 29.22 |
| | CC+Pantheon+ | 1644.828 | 1642.044 | 1656.828 | 1648.044 | 1689.570 | 1664.204 | 8.784 | 25.366 |
| II | CC | 38.912 | 32.132 | 50.912 | 38.132 | 59.515 | 42.431 | 12.78 | 17.08 |
| | Pantheon+ | 1595.117 | 1609.917 | 1607.117 | 1615.917 | 1639.750 | 1632.231 | 8.8 | 7.519 |
| | CC+Pantheon+ | 1634.029 | 1642.044 | 1646.029 | 1648.044 | 1678.771 | 1664.204 | 2.015 | 14.567 |

ures the global evolution history of $H(z)$; hence, only after *Om* diagnosis can we suggest that our model behavior is indeed phantom.

In general, both models indicate that they are globally in the phantom region.

### B. Statefinder Diagnostics

Although *Om* diagnostics is an excellent null test, it has several problems; for example, it does not distinguish between various types of quintessence and phantom models. Moreover, the formula is too simple, so it does not take into account the nuances of the other types of late cosmology and how much they differ from ΛCDM.

To circumvent these issues, Sahni *et al*. [82] proposed a null test based on two different parameters, $r, s$, given by the formulas

$$r = \frac{\dddot{a}}{aH^3} \tag{73}$$

and

$$s = \frac{r-1}{3\left(q-\frac{1}{2}\right)}. \tag{74}$$

First, note that, for the standard ΛCDM model, $q=-1$; hence, $r=0$. Consequently, an advantage of $r$ is that, although various models give similar $H$ and $q$, they differ by the third derivative. In other words, $r$. $s$ is defined to distinguish between various forms of dark energy models. Together, $r$ and $s$ can distinguish between various models, such as those of Chaplygin gas, phantom, and quintessence. Therefore, it can be easily shown that, for ΛCDM $(\omega=-1)$, $s=0, r=1$. However, $s<0$ and $r>1$ (for both of our models) are phantom in nature. This also shows that our current universe $(z\approx 0)$ is located in the phantom region and will eventually converge to ΛCDM. It is worth noting that statefinder diagnosis alone cannot distinguish between brane world and Chaplygin gas, and we cannot say for certain which dark energy model is represented, except that it is neither "pure quintessence" nor a time-independent equation of state (*i.e.,* $\dot{\omega}\neq 0$). For a scalar field-based dark energy model, the statefinder, or more precisely $s$, does not uniquely specify the models. For example, a detailed analysis of the behavior with respect to the phantom [83], interacting phantom [84], and quintom fields [85] reveals how the statefinder generally changes for all these potentials.

## X. CONCLUSION

In this study, we propose a unified model of dark energy and dark matter via the (generalized) Chaplygin gas model. We show that an MCMC analysis with both the Hubble and Pantheon+SH0ES datasets favors an MOG dark energy ($m\approx -5$) and dark matter ($m\approx= -2$) dominated universe (dark energy originating from the MOG part). To systematically account for the transition, we employ a standard interaction term $\mathcal{I}$, which can serve as a mediator between dark matter and dark energy. Overall, we show that data analysis (ΔAIC and ΔBIC tests) favors the BEC dark-matter model over dark energy when using the pure Chaplygin gas model.

Here is a brief overview of the final results presented in this manuscript. First, in Figs. 1 and 2, we present least squares fitting for the Hubble and supernova datasets and compare the Chaplygin gas ($m\approx -5$) and BEC ($m\approx 2$) models with the standard ΛCDM model to show the insignificant deviation between the two. This shows that, phenomenologically, our model is consistent with the current observation. Fig. 3 shows the results of the MCMC analysis; a $3\sigma$ contour plot is plotted using the corner plot in the EMCEE package in Python. Similarly, as shown in Fig. 4, we perform the same analysis for BEC dark matter and find that $m\approx 2$ is also a valid solution, which produces a late-time de Sitter solution. Note that the obtained constraint $n\neq 1$ does not contradict the standard GR tests, which allows for consistency between the MOG model and the data. Similar observations can be obtained in the context of $f(R)$ gravity and also when adjusting it with large scale structures, X-rays [86], or UV-flux datasets [87]. This is analogous to the $f(R)$ gravity case at lower scales, such as the Solar System or Shapiro time-delay-like experiments, where a screening mechanism adjusts the gravity to ensure it is consistent with the Einstein Hilbert action (as discussed in detail by Weltman et. al [88] and Harko *et al*. [89]). Figs. 5 and 7 show the behaviors of phenomenological quantities such as $q$ and $\omega_{\rm eff}$ for $m\approx -5$ and $m=2$, respectively. As expected, both exhibit late time de Sitter behavior (*i.e.*, at $z\to -1$, $q, \omega_{\rm eff}\to -1$). Finally, Figs. 6 and 8 show the results of the two most famous null-tests for the ΛCDM model, that is, statefinder and Om diagnostics, both of which indicate phantom behavior in the current time and late-time de Sitter transition. This reveals the consistency of our model with the current paradigm.

Moreover, as listed in Table 3, after qualitatively examining ΔAIC and ΔBIC, our model is found to favor the BEC model over the Chaplygin gas model, confirming that there is a nontrivial interaction term between the two.

Here, we provide a brief outline of the entire paper.

First, we begin with the introduction (Section-I), where we detail our motivation for considering the Chaplygin gas equation of state as a unification of both dark matter and dark energy. We explain why Chaplygin gas models are appealing: they naturally occur in string theory and connect between a matter-dominated and dark-energy-dominated universe. We also discuss how

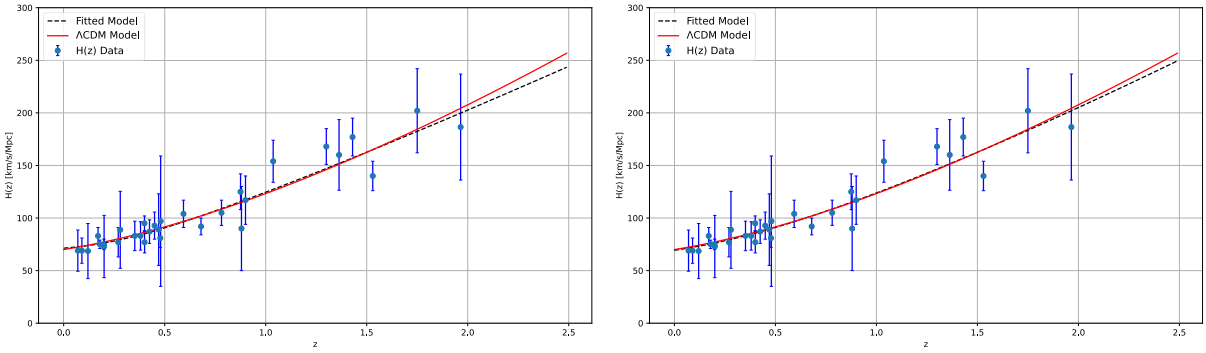


**Fig. 1.** (color online) Least squares fitting for the Chaplygin gas model (left panel as dark energy $m \approx -5$ and right panel as BEC dark matter $m \approx 2$). The standard ΛCDM model (black dashed line) is compared with our proposed model fitted with the Hubble function $H(z)$ versus redshift $z$ (red line). An error bar plot representing the 31 CC dataset points considered for the analysis is also included.

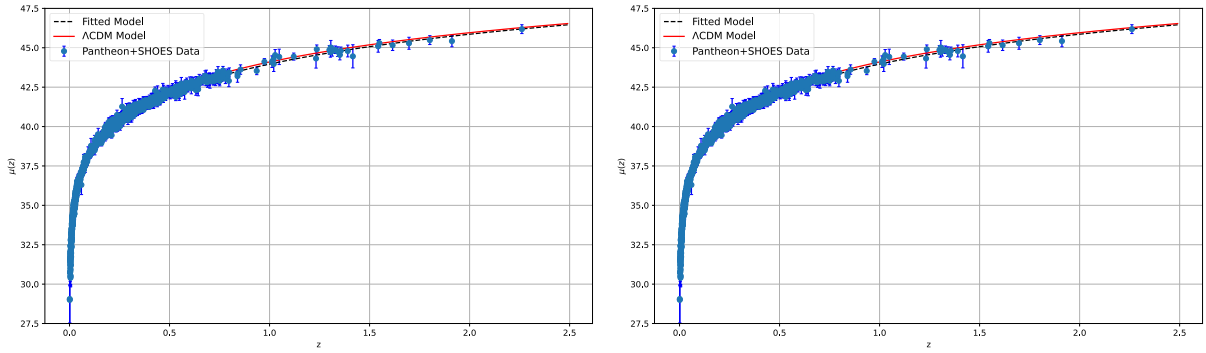


**Fig. 2.** (color online) Least squares fitting for the Chaplygin gas model (left panel as dark energy $m \approx -5$ and right panel as BEC dark matter $m \approx 2$). The standard ΛCDM model (black dashed line) is compared with our proposed model fitted with the function $\mu(z)$ versus redshift $z$ (red line). An error bar plot representing the 1701 points of the Pantheon+SH0ES dataset considered for the analysis is also included.

the Bose-Einstein condensate could be a dark-matter candidate and the motivation for including the interaction term between dark matter and dark energy. After giving a brief outline of symmetric teleparallel-based gravity, we perform data analysis and null-tests (Om and statefinder diagnosis).

In Section II, we present a more detailed discussion on Chaplygin gas and show how various microscopic theories, such as the scalar field, DBI field, and brane world scenarios, can give rise to the Chaplygin gas equation of state. This section also serves as a primer indicating that the best fit for the Chaplygin gas model can be used to reconstruct the scalar field potential, DBI field potential, and even the wrapping factor for branes. Therefore, we demonstrate the universality of the Chaplygin gas model from both the microscopic and phenomenological perspectives.

In Section III, we discuss how dark matter can be modeled using BEC. We provide a brief physical motivation: the universe's state of formation could create an ideal environment for BEC to occur. BEC could explain the uniform density of dark-matter halos and is also an effective theory because, regardless the identity of the underlying bosons, if they are massive, there is a possibility for BEC. We also discuss the microscopic origin of BEC using the Gross-Pitaevskii equations for a weakly interacting Bose gas. Subsequently, we argue that the variation in such an energy function could lead to the Chaplygin gas equation-like form. Overall, this gives a microscopic and observationally sound reason for modeling dark matter as a Bose-Einstein condensate.

In Section IV, we advocate for a uniform framework for dark matter and dark energy, arguing that the values of $m$ can be used to easily verify the domination of the model by dark energy, as described by the Chaplygin gas equation or BEC dark matter. We also discuss the need to include an interaction term to allow for consistency with the standard model of cosmology and to maintain the ratios of dark matter and dark energy.

In Section V, we give a brief description of $f(Q)$ gravity. We discuss the gauge choice and the reason why the boundary term does not impact the formulation. We then take a brief detour to explain a method of calculating the non-metric scalar from $Q_{\alpha\mu\nu}$. In Section VI, we continue the discussion on $f(Q)$ gravity under the FLRW metric, taking a flat FLRW metric with signature $(-+++)$ and providing a way to calculate the non-metric scalar, which is found to be $6H^2$. We also argue that $f(Q) = -Q$

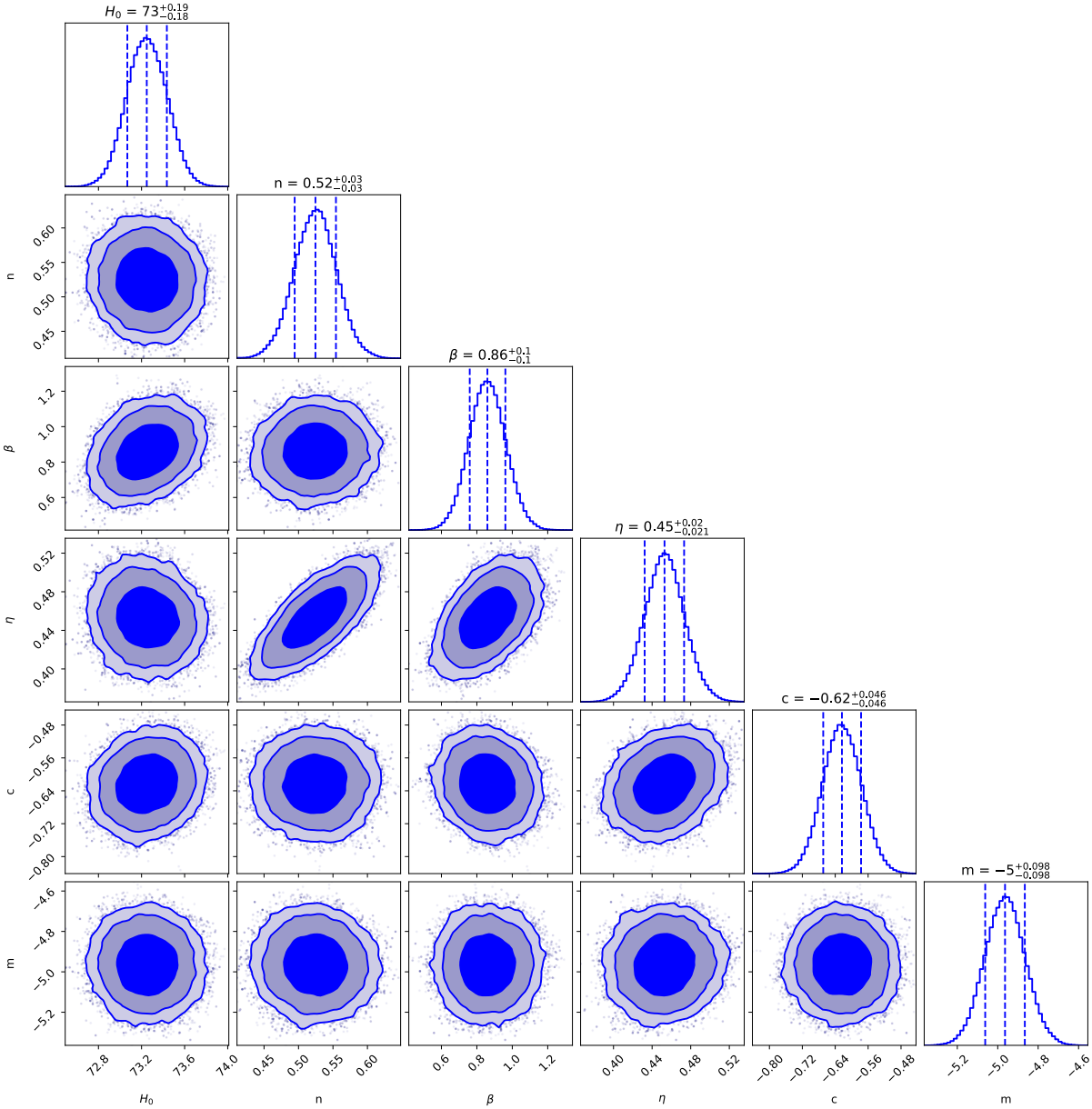


**Fig. 3.** (color online) MCMC analysis for the Chaplygin gas model (as dark energy $m \approx -5$). Based on a combined examination of the CC, BAO, and Pantheon+SH0ES datasets, the 2D-contour plot of the model parameters $m$, $c$, $\eta$, $\beta$, $n$, and $H_0$ displays the most likely values and confidence areas up to $3-\sigma$.

can facilitate Einstein GR, providing a consistency check between MOG and standard Einstein GR.

In Section VII, we provide the complete formula for $H(z)$ as a function of $z$ (redshift), using the continuity equation and Friedmann equation to arrive at an exact formula. This enables us to perform data analysis and constrain the free parameters.

In Section VIII, we perform a complete data analysis using the formula for $H(z)$. We find two models: Model I ($m \approx -5$) and Model II ($m \approx 2$), both of which yield constant observational values. Both models have similar $q$ and $\omega$, closely resembling our current universe's observational data. Although both models give observably constant results and satisfy the null tests, Model II, which is dark matter dominated, gives the lowest Δ AIC and Δ BIC, indicating that Chaplygin gas is more biased toward dark matter modeled by BEC. This also suggests that there is a non-trivial (as $b \neq 0$) interaction between dark matter and dark energy, that is, dark matter is transformed into dark energy.

In Section IX, we perform two popular null tests for the ΛCDM model, namely, the Om and statefinder diagnoses. Both investigated models under the Om diagnosis approach the standard ΛCDM model while currently

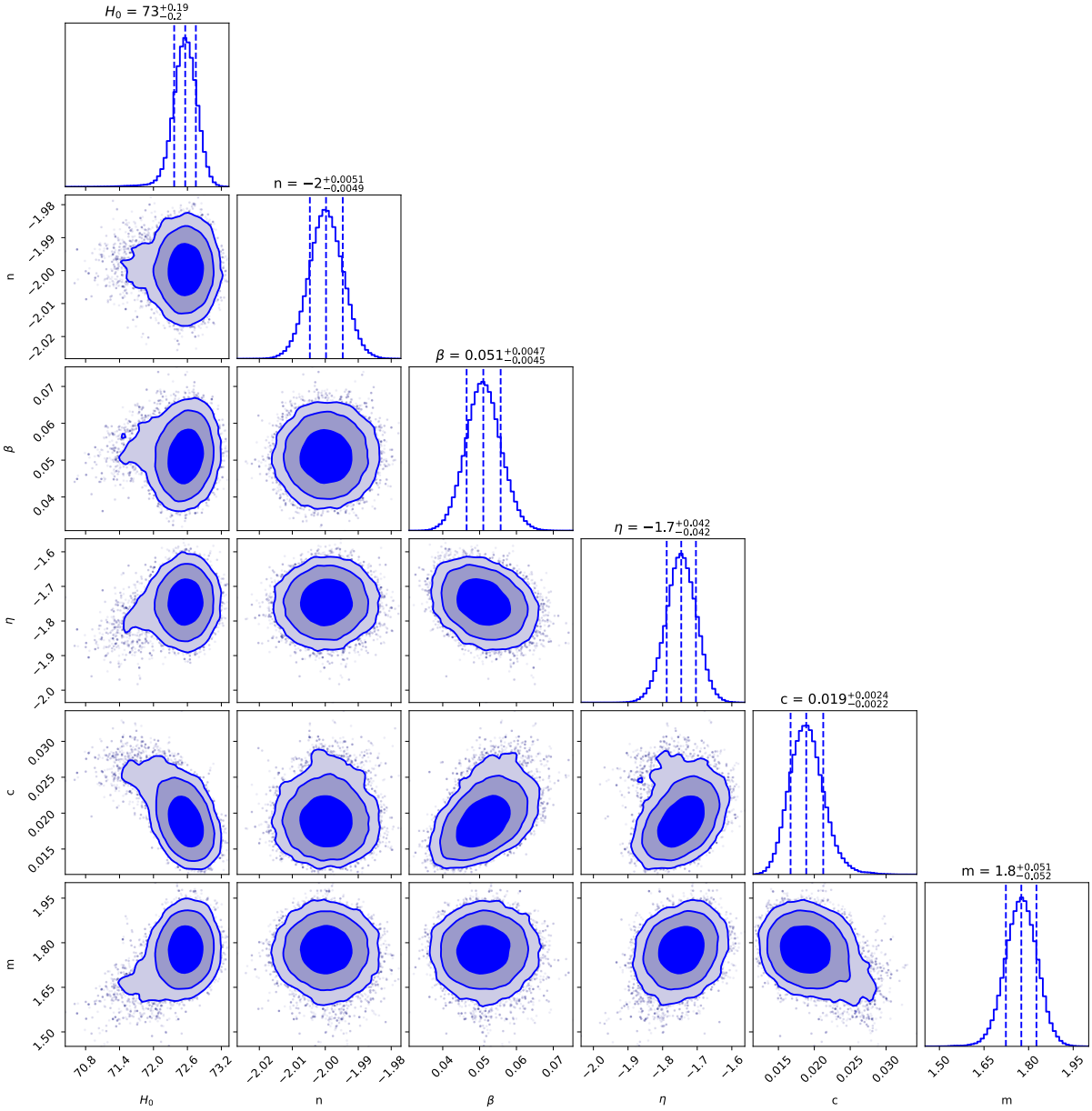


**Fig. 4.** (color online) MCMC analysis for the Chaplygin gas model (as BEC dark matter $m \approx 2$). Based on a combined examination of the CC, BAO, and Pantheon+SH0ES datasets, the 2D-contour plot of the model parameters $m$, $c$, $\eta$, $\beta$, $n$, and $H_0$ displays the most likely values and confidence areas up to $3-\sigma$.

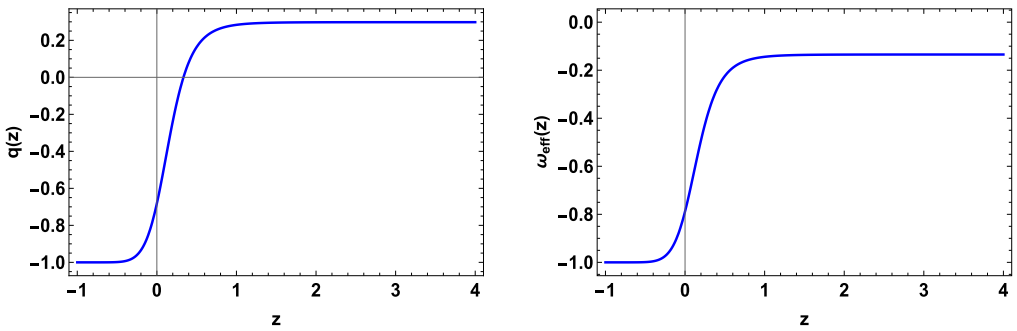


**Fig. 5.** (color online) Deceleration parameter $q(z)$ and effective equations of state $\omega(z)$ for the Chaplygin gas model (as dark energy $m \approx -5$). Both converge to $-1$ at $z \to -1$, as expected, which is highly consistent with the current values of the observed $q$ and $\omega$.

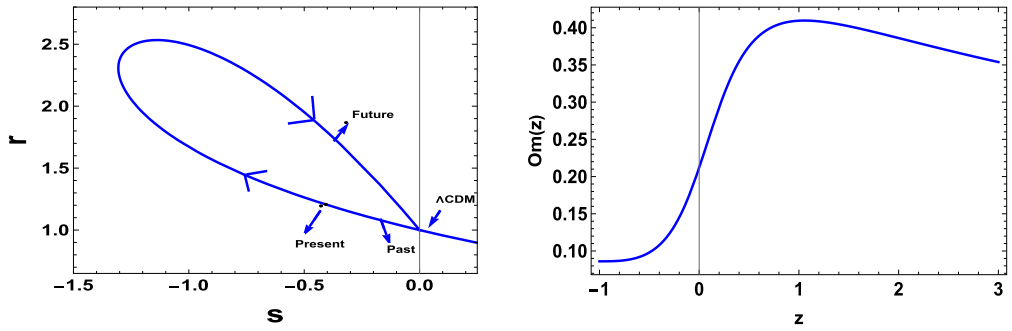


**Fig. 6.** (color online) To check the models, we use two popular null tests for the ΛCDM model. First, we construct the $r-s$ plot, which shows late-time convergence to the ΛCDM model. We also use *Om* diagnostics to test the variation from ΛCDM for the Chaplygin gas model (as dark energy $m \approx -5$).

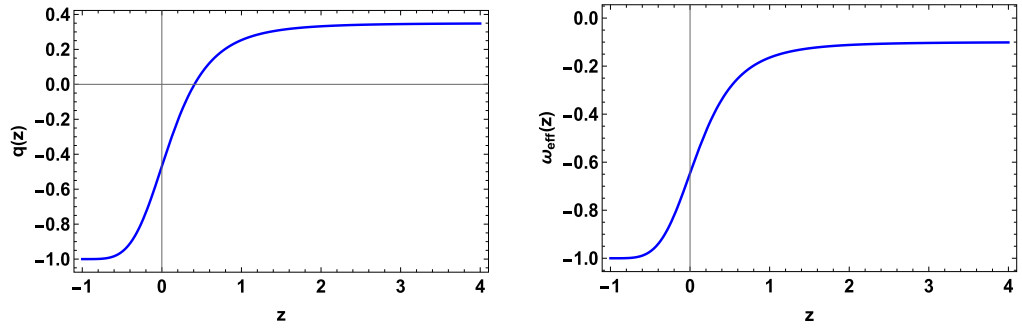


**Fig. 7.** (color online) Deceleration parameter $q(z)$ and effective equations of state $\omega(z)$ for the Chaplygin gas model (as dark matter $m \approx 2$). Both converge to $-1$ at $z \to -1$, as expected, which is highly consistent with the current values of the observed $q$ and $\omega$.

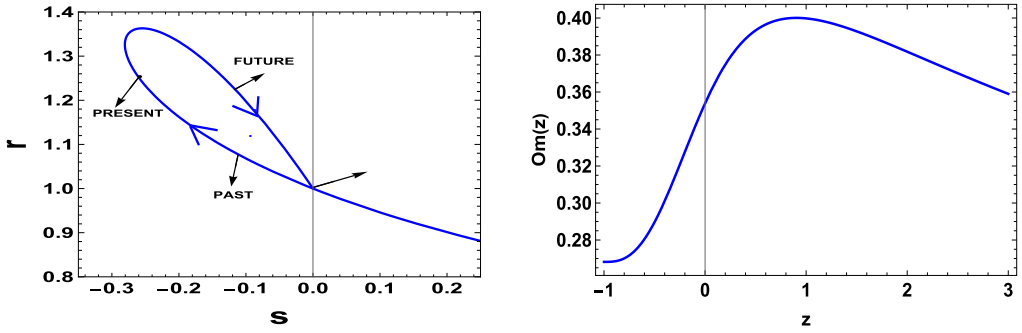


**Fig. 8.** (color online) To check the models, we use two popular null tests for the ΛCDM model. First, we construct the $r-s$ plot, which shows late-time convergence to the ΛCDM model. We also use *Om* diagnostics to test the variation from ΛCDM for the Chaplygin gas model (as BEC dark matter $m \approx 2$).

passing through the phantom epoch. In terms of the statefinder diagnosis, the results are also consistent with the phantom behavior; however, it could also denote any other form of the scalar fields, as mentioned above. This is unsurprising, as the Chaplygin gas equation of state typically gives phantom behavior. As shown in Section II, a non-standard kinetic energy term is required to arrive at the Chaplygin gas equation of state.

Finally, Section X presents the conclusion. Overall, this study demonstrates that a unified framework for dark matter and dark energy can be obtained through the Chaplygin gas model in $f(Q)$ MOG, and data analysis yields tight observational constraints on the free parameters. This study can be extended by using more general MOG models, such as $f(Q,T), f(Q,B), f(Q,T)$, or general $f(Q,T,L_m)$ models, to ascertain whether the conclusions of our models are empirical.

## ACKNOWLEDGMENTS

*We are very grateful to the honorable referee and editor for their illuminating suggestions, which have signi-*

*ficantly improved our work in terms of research quality and presentation.*

There are no new data associated with this article.

## References


[1] A. G. Riess *et al*. (Supernova Search Team), Astron. J. **116**, 1009 (1998)
[2] S. Perlmutter *et al*. (Supernova Cosmology Project Collaboration), Astrophys. J. **517**, 565 (1999)
[3] J. E. Taylor and J. Silk, Mon. Not. R. Astron. Soc. **339**, 505 (2003)
[4] R. Massey, T. Kitching, and J. Richard, Rep. Prog. Phys. **73**, 086901 (2010)
[5] M. Blau and S. Theisen, Gen. Relativ. Gravit. **41**, 743 (2009)
[6] M. Bojowald, Class. Quantum Grav. **29**, 213001 (2012)
[7] G. Simpson, K. Bolejko, and S. Walters, Class. Quantum Grav. **42**, 145001 (2025)
[8] L. Kazantzidis and L. Perivolaropoulos, Phys. Rev. D **97**, 103503 (2018)
[9] A. A. Starobinsky, Phys. Lett. B **91**, 99 (1980)
[10] U. Das and B. Mukhopadhyay, Phys. Rev. Lett. **110**, 071102 (2013)
[11] C. S. J. Pun, Z. Kovács, and T. Harko, Phys. Rev. D **78**, 024043 (2008)
[12] J. B. Jiménez, L. Heisenberg, and T. Koivisto, Phys. Rev. D **98**, 044048 (2018)
[13] J. B. Jiménez, L. Heisenberg, and T. S. Koivisto, JCAP **08**, 039 (2018)
[14] J. B. Jiménez, L. Heisenberg, and T. S. Koivisto, Universe **5**, 173 (2019)
[15] A. Mussatayeva, N. Myrzakulov, and M. Koussour, Phys. Dark Univ. **42**, 101276 (2023)
[16] M. Koussour, N. Myrzakulov, A. H. A. Alfedeel *et al*., Prog. Theor. Exp. Phys. **2023**, 113E (2023)
[17] M. Koussour and A. De, Eur. Phys. J. C **83**, 400 (2023)
[18] N. Myrzakulov, M. Koussour, A. Mussatayeva, Chin. J. Phys. **85**, 345 (2023)
[19] M. Koussour, S. H. Shekh, and M. Bennai, J. High Energy Astrophys. **35**, 43 (2022)
[20] M. Koussour, S. H. Shekh, A. Hanin *et al*., Class. Quantum Gravity **39**, 195021 (2022)
[21] S. Ghosh, R. Solanki, and P. K. Sahoo, Phys. Scr. **99**, 055021 (2024)
[22] S. Ghosh, R. Solanki, and P. K. Sahoo, Chin. Phys. C **48**, 095102 (2024)
[23] D. J. Gogoi, A. Övgün, and M. Koussour, Eur. Phys. J. C **83**, 700 (2023)
[24] Z. Hassan, S. Ghosh, P. K. Sahoo *et al*., Eur. Phys. J. C **82**, 1116 (2022)
[25] Z. Hassan, S. Ghosh, P. K. Sahoo *et al*., Gen. Rel. Grav. **55**, 90 (2023)
[26] D. Mohanty, S. Ghosh, and P. K. Sahoo, Ann. Phys. **463**, 169636 (2024)
[27] D. Mohanty, S. Ghosh, and P. K. Sahoo, Int. J. Mod. Phys. D **34**, 2550041 (2025)
[28] L. Amendola, Phys. Rev. D **62**, 043511 (2000)
[29] G. R. Farrar and P. J. E. Peebles, Astrophys. J. **604**, 1 (2004)
[30] W. Zimdahl and D. Pavon, Class. Quantum Grav. **24**, 5461 (2007)
[31] Yu. L. Bolotin, A. Kostenko, O. A. Lemets *et al*., Int. J. Mod. Phys. D **24**, 1530007 (2014)
[32] B. Wang, E. Abdalla, F. Atrio-Barandela *et al*., Rep. Prog. Phys. **79**, 096901 (2016)
[33] A. Bhat, R. Solanki, and P. K. Sahoo, Gen. Relativ. Gravit. **56**, 63 (2024)
[34] A. Kamenshchik, U. Moschella, and V. Pasquier, Phys. Lett. B **511**, 265 (2001)
[35] M. C. Bento, O. Bertolami, and A. Sen, Phys. Rev. D **66**, 043507 (2002)
[36] A. Kamenshchik, U. Moschella, and V. Pasquier, Phys. Lett. B **487**, 7 (2000)
[37] S. K. Kama, Phys. Lett. B **424**, 39 (1998)
[38] M. Novello, M. Makler, L. S. Werneck *et al*., Phys. Rev. D **71**, 043515 (2005)
[39] H. Benaoum, Universe **8**, 340 (2022)
[40] D. Carturan and F. Finelli, Phys. Rev. D **68**, 103501 (2003)
[41] O. Bertolami, A. A. Sen, S. Sen *et al*., Mon. Not. R. Astron. Soc. **353**, 329 (2004)
[42] M. Makler, S. Quinet de Oliveira, and I. Waga, Phys. Lett. B **555**, 1 (2003)
[43] M. C. Bento, O. Bertolami, and A. A. Sen, Phys. Lett. B **575**, 172 (2003)
[44] A. Dev, D. Jain, and J. S. Alcaniz, Phys. Rev. D **67**, 023515 (2003)
[45] J. S. Alcaniz, D. Jain, and A. Dev, Phys. Rev. D **67**, 043514 (2003)
[46] J. V. Cunha, J. A. S. Lima, and J. S. Alcaniz, Phys. Rev. D **69**, 083501 (2004)
[47] L. Randall and R. Sundrum, Phys. Rev. Lett. **83**, 3370 (1999)
[48] C. C. Bradley, C. A. Sackett, J. J. Tollett *et al*., Phys. Rev. Lett. **75**, 1687 (1995)
[49] C. G. Boehmer and T. Harko, JCAP **06**, 025 (2007)
[50] T. Harko, Phys. Rev. D **83**, 123515 (2011)
[51] T. Harko and F. S. N. Lobo, Phys. Rev. D **92**, 043011 (2015)
[52] Y. Mambrini, S. Profumo, and F. S. Queiroz, Phys. Lett. B **760**, 807 (2016)
[53] D. Hooper and S. Profumo, Phys. Rep. **453**, 29 (2007)
[54] S. S. Mishra and V. Sahni, JCAP **04**, 007 (2020)
[55] S. D. Odintsov and V. K. Oikonomou, Phys. Rev. D **99**, 104070 (2019)
[56] S. Das and R. K. Bhaduri, (2018), arXiv: 1812.07647[gr-qc]
[57] S. Das and S. Sur, Phys. Dark Univ. **42**, 101331 (2023)
[58] E. Mahichi, A. Amani, and M. A. Ramzanpour, Can. J. Phys. **99**, 11 (2021)
[59] E. Mahichi, A. Amani, and M. A. Ramzanpour, Mod. Phys. Lett. A **37**, 2250228 (2022)
[60] E. Mahichi and A. Amani, Phys. Dark Univ. **39**, 101167 (2023)
[61] M. R. Setare, J. Sadeghi, and A. R. Amani, Phys. Lett. B **673**, 241 (2009)
[62] L. P. Chimento, A. S. Jakubi, D. Pavon *et al*., Phys. Rev. D **67**, 083513 (2003)
[63] Z. K. Guo, Y. S. Piao, X. M. Zhang *et al*., Phys. Lett. B **608**, 177 (2005)
[64] L. Heisenberg, Phys. Rep. **1066**, 1 (2024)

[65] F. D'Ambrosio, L. Heisenberg, and S. Kuhn, Class. Quantum Grav. **39**, 025013 (2022)
[66] S. W. Hawking and G. F. R. Ellis, *The Large Scale Structure of Space-Time*, First edition (Cambridge University Press, 1973), p.135
[67] J. Einasto et. al., Astron. Astrophys. **462**, 397 (2006)
[68] Planck Collaboration, *A&A*, **641 A(6)**: 1-67 (2020).
[69] M. Moresco, Mon. Not. Roy. Astron. Soc. **463**, L6 (2016)
[70] R. Solanki, S. K. J. Pacif, A. Parida *et al*., Phys. Dark Univ. **32**, 100820 (2021)
[71] R. Solanki, A. De, S. Mandal *et al*., Phys. Dark Universe **36**, 101053 (2022)
[72] M. Kowalski *et al*. (Supernova Cosmology Project Collaboration), Astrophys. J. **686**, 749 (2008)
[73] R. Amanullah, C. Lidman, D. Rubin *et al*., Astrophys. J. **716**, 712 (2010)
[74] N. Suzuki *et al*. (Supernova Cosmology Project Collaboration), Astrophys. J. **746**, 85 (2012)
[75] M. Betoule *et al*. (SDSS Collaboration), Astron. Astrophys. **568**, A22 (2014)
[76] D. M. Scolnic *et al*. (Pan-STARRS1 Collaboration), Astrophys. J. **859**, 101 (2018)
[77] D. Scolnic, D. Brout, A. Carr *et al*., Astrophys. J. **938**, 113 (2022)
[78] H. Akaike, IEEE Trans. Autom. Control **19**, 716 (1974)
[79] G. Schwarz, Ann. Statist. **6**, 461 (1978)
[80] A. R. Liddle, Mon. Not. Roy. Astron. Soc. **377**, L74 (2007)
[81] V. Sahni, A. Shafieloo, and A. A. Starobinsky, Phys. Rev. D **78**, 103502 (2008)
[82] V. Sahni, T. D. Saini, A. A. Starobinsky *et al*., JETP Lett. **77**, 201 (2003)
[83] P. X. Wu and H. W. Yu, Mod. Phys. Lett. A **21**, 1305 (2006)
[84] B. Chang, H. Liu, L. Xu *et al*., JCAP **01**, 016 (2007)
[85] P. X. Wu and H. W. Yu, Int. J. Mod. Phys. D **14**, 1873 (2005)
[86] L. Lombriser, A. Slosar, U. Seljak *et al*., Phys. Rev. D **85**, 124038 (2012)
[87] M. Leizerovich, L. Kraiselburd, S. Landau *et al*., Phys. Rev. D **105**, 103526 (2022)
[88] J. Khoury and A. Weltman, Phys. Rev. Lett. **93**, 171104 (2004)
[89] T. Harko, F. S. N. Lobo, S. Nojiri *et al*., Phys. Rev. D **84**, 024020 (2011)